Available online at www.sciencedirect.com
ScienceDirect
Journal of Luminescence 128 (2008) 818–820
JOURNAL OF LUMINESCENCE
www.elsevier.com/locate/jlumin

Investigation on the improvement of red phosphorescence in $CaTiO_3:Pr^{3+}$ nanoparticles

Xianmin Zhang[a,b], Jiahua Zhang[a,1], Meiyuan Wang[a,b], X. Zhang[a], H. Zhao[a], Xiao-Jun Wang[a,c,*]

[a]*Key Laboratory of Excited State Processes, Changchun Institute of Optics, Fine Mechanics and Physics, Chinese Academy of Sciences, 16 Eastern South Lake Road, Changchun 130033, China*
[b]*Graduate School of Chinese Academy of Sciences, Beijing 100039, China*
[c]*Department of Physics, Georgia Southern University, Statesboro, GA 30460, USA*

Available online 8 December 2007

Abstract

Red phosphorescence in nanosized $CaTiO_3:Pr^{3+}$ phosphors has been investigated by measuring the spectra of emission and excitation, as well as the charging and decay processes. The emission intensity and the persistent time have been improved. More energy traps have been observed in nanoparticles compared to the bulk powders. The integral emission intensity from the nanoparticles is remarkably greater than that from the bulk. A phosphorescence recombination mechanism through tunneling in nanoparticles is discussed.

Keywords: $CaTiO_3:Pr^{3+}$; Phosphorescence; Nanoparticles

1. Introduction

The achievement of intense red-emitting persistent phosphors is one of the challenging goals in the field of display and lighting technologies [1,2]. Recently, much work has been concentrated on the novel red-emitting phosphors of Pr^{3+}-doped $CaTiO_3$ [3–6]. In order to enhance the phosphorescence emission, some metal oxides, such as MgO or ZnO [3], Al_2O_3 [5], and Lu_2O_3 [6] are co-doped in the host to increase the number of traps. We reported the enhancement of red phosphorescence in $CaTiO_3:Pr^{3+}$ nanoparticles due to the existence of more traps contributing to phosphorescence in the nanoparticles [7]. The work suggested a new direction for developing long-lasting phosphor by manipulating the surface traps of nanoscaled materials. However, the recombination mechanism of phosphorescence in $CaTiO_3:Pr^{3+}$ nanoparticles and the effect of surface traps on the fluorescence and phosphorescence are not yet well understood. In the present work, the further investigation has been made in detail by measuring and comparing the charging and release processes. The results suggest that the released electrons or holes are recombined through tunneling rather than the conduction band or the valence band with the active centers in nanoparticles.

2. Experimental section

A 0.01 M $CaCl_2$, 0.01 M citric acid–ethanol solution and $PrCl_3$ solution (Pr_6O_{11} was dissolved in HCl) were mixed. The molar ratio of Ca^{2+} to Pr^{3+} was 1:0.4%. Under constant magnetic stirring, $Ti(OC_4H_9)_4$ was slowly added until an yellow sol was obtained. By heating the yellow sol at 100 °C for 10 h, the sol changed to gel. After further firing the gel at 300 °C for 2 h, a dark solid mass was obtained. When it was cooled to room temperature, it was ground into powder. White nanosized $CaTiO_3:Pr^{3+}$ particles were obtained after sintering the black powder at different sintering temperatures for 2 h in air. The bulk

*Corresponding author at: Key Laboratory of Excited State Processes, Changchun Institute of Optics, Fine Mechanics and Physics, Chinese Academy of Sciences, 16 Eastern South Lake Road, Changchun 130033, China. Tel./fax: +86 431 8617 6317.
E-mail addresses: zjiahua@public.cc.jl.cn (J. Zhang), xwang@georgiasouthern.edu (X.-J. Wang).
[1]Also for correspondence. Tel./fax: +86 431 8617 6317.

0022-2313/$ - see front matter © 2008 Elsevier B.V. All rights reserved.
doi:10.1016/j.jlumin.2007.12.010

powders (the molar ratio of Ca^{2+} to Pr^{3+} was 1:0.1%) were synthesized by conventional solid-state reaction at 1400 °C for 3 h in air. The structure of the products was characterized by powder X-ray diffractometer using a Cu target radiation source. Photoluminescence (PL), PL excitation (PLE), diffused spectra ($BaSO_4$ powders were used as a standard) and afterglow decay curves were measured using a Hitachi F-4500 fluorescence spectrophotometer. The samples were kept in dark for 48 h before starting the charging process.

3. Results and discussion

X-ray diffraction (XRD) patterns of $CaTiO_3$:Pr^{3+} nanoparticles (a–c) at various sintering temperatures and bulk powders (d) are shown in Fig. 1. Compared to the bulk sample, it is found that the $CaTiO_3$ phase for the nanoparticles has been well formed at 500 °C. The phase of the bulk is orthorhombic (JCPDS Card no. 82-0228). There are no extra peaks from nanoparticles, suggesting a single phase that is consistent with the bulk. By applying the Scherrer formula to the full-width at half-maximum of the diffraction peaks, the mean particle size is calculated to be 12.5 nm for sample b and 27.5 nm for sample c.

The PL and PLE spectra of $CaTiO_3$:Pr^{3+} nanoparticles and bulk powders are depicted in Fig. 2. The quenching concentration of Pr^{3+} in $CaTiO_3$ is 0.4% for the nanoparticles and 0.1% for bulk powders [7]. The red emission at 615 nm shown in PL spectra is attributed to the intra-4f $^1D_2$–$^3H_4$ transitions of Pr^{3+} [4]. The PLE spectra monitoring the red emission mainly consists of two broad

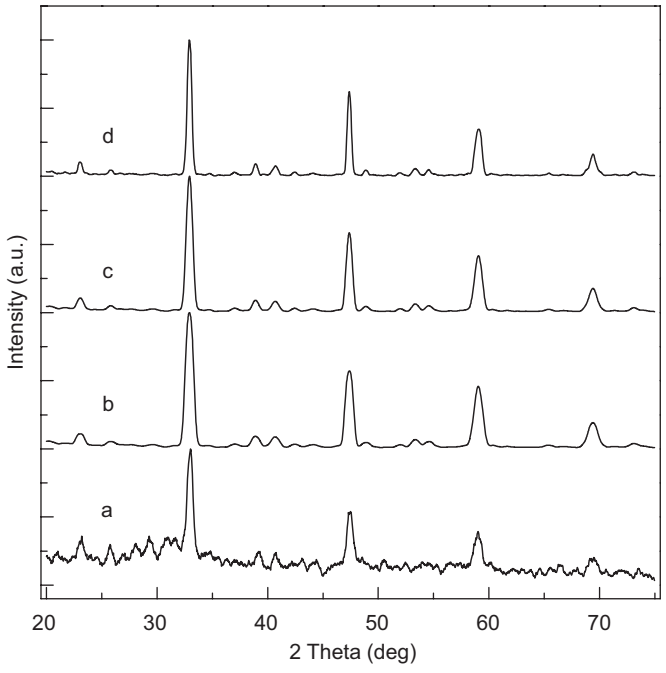

Fig. 1. XRD patterns of $CaTiO_3$:Pr^{3+} for nanoparticles at different sintering temperatures and bulk powders: (a) 400 °C; (b) 500 °C; (c) 600 °C for 2 h and (d) bulk powders.

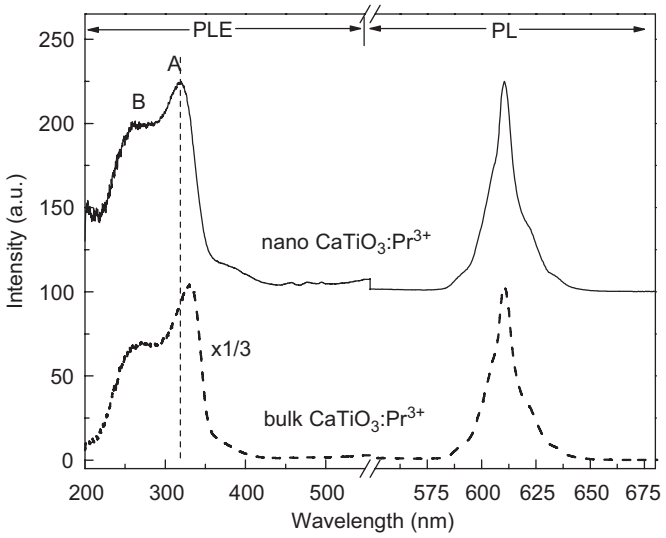

Fig. 2. PL and PLE spectra of $CaTiO_3$:Pr^{3+} for nanoparticles (sample c) and bulk powders.

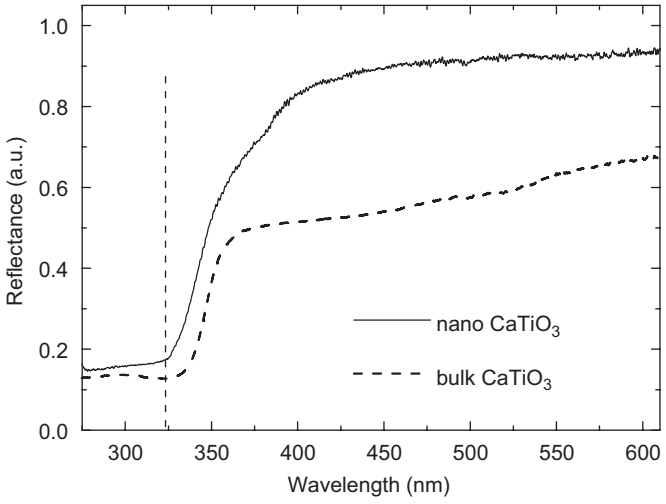

Fig. 3. Diffused reflectance spectra of $CaTiO_3$ host for the nanoparticles (solid line) and bulk powders (dashed line).

bands in the ultraviolet region, which are located at 319 nm (A) and 265 nm (B), respectively. In comparison with the PLE spectra of $CaTiO_3$:Pr^{3+} bulk powders (dashed line), band A shifts from 330 nm in the bulk to 319 nm in the nanoparticles. The position of band A is observed to be consistent with that of the band edge absorption of $CaTiO_3$ host due to O(2p)-Ti(3d) transition [4] (see Fig. 3), indicating that the blue shift of band A in the nanoparticles is due to the size-confinement effect. This effect has also been reported in $CaTiO_3$:Pr^{3+} thin films [8]. The band B is attributed to the $4f^2 \rightarrow 4f^5d$ absorption of Pr^{3+} ions [4,5].

The diffused reflectance spectra of the host for the nanoparticles (solid line) and the bulk (dashed line) powders are presented in Fig. 3. The valence-to-conduction absorption bands with edge around 319 nm for nanoparticles and 330 nm for bulk powders are observed. The blue

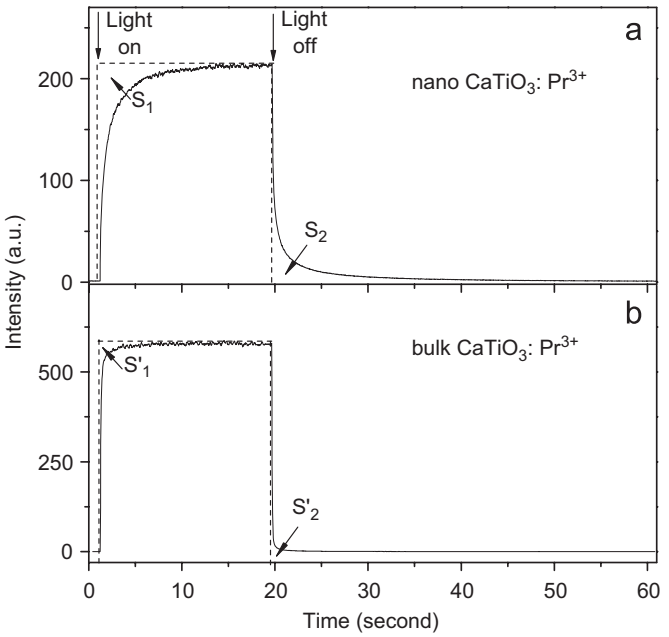

Fig. 4. The charging (at 365 nm) and release processes of $CaTiO_3:Pr^{3+}$ nanoparticles (sample c) and the bulk powders. S_1, S'_1, and S_2, S'_2 represent the stored energy and released energy for (a) nanoparticles and (b) bulk powders, respectively.

shift of host absorption due to the size effect in nanoparticles is clearly shown, which is consistent with the PLE spectra (Fig. 2). The enhancement of reflectance in nanoparticles in comparison with that of the bulk powders is also observed. The reason is that, for the bulk, there exist some point defects, such as Ca and Ti vacancy defects [9], when prepared at high temperatures (~1400 °C). These defects act as a color center, absorbing visible light and decreasing the reflectance. The defects will not be created at low temperature (600 °C), where the nanoparticle samples are prepared by the sol–gel method. So the body color of the nanoparticles is white, while the bulk is gray. It should be noted that these vacancy defects acting as nonradiative centers reduce the fluorescence and phosphorescence efficiency of $CaTiO_3:Pr^{3+}$ phosphors [6,9].

The optical charging and releasing processes under the same irradiation density for red phosphorescence in nanosized $CaTiO_3:Pr^{3+}$ phosphors in comparison with the bulk powders are illustrated in Fig. 4. The areas (S_1 for the nano-samples and S'_1 for the bulk) above the charging curve and below the dashed lines represent the energy stored in the traps [10]. It is found that S_1 is much greater than S'_1, indicating more energy stored in nanophosphors than that in the bulk, although the fluorescence in nanophosphors is weaker than that of the bulk. The capability of energy storing is related to the number of traps [11]. The enhancement of the energy storing and the phosphorescence is a reflection of the increase of the traps. The integral intensity of the phosphorescence (proportional to the area S_2) after excitation in nanoparticles is remarkably larger than that of the bulk (proportional to the area S'_2), further approving that there exist more trapping centers in the nanoparticles. It can be deduced that a large amount of surface traps due to large surface-to-volume ratio in the nanoparticles benefit the phosphorescence, although part of the surface defects acting as nonradiative centers quench the fluorescence efficiency. Therefore, in nanoparticles, it can be assumed that there exists another phosphorescent recombination channel, such as tunneling, which has higher transfer efficiency than that of the recombination through the conduction band for an electron trap or the valence band for a hole trap. Thus, the efficiency of the phosphorescence remains very high. This is supported by the fact that area S_1 and S_2 are nearly the same, showing that the recombination rate of phosphorescence is little affected by the nonradiative centers in nanoparticles mentioned above. The tunneling model for the decay of the phosphorescence has been proposed for other systems, such as Zn_2SiO_4:Mn phosphors [12].

4. Conclusions

In conclusion, the enhancement of the phosphorescence and the reduction of the fluorescence in $CaTiO_3:Pr^{3+}$ nanoparticles in comparison with the bulk powders are observed. Based on the analysis of charging and release processes as well as the fluorescence emission efficiency, a tunneling recombination mechanism for phosphorescence in nanoparticles is assumed.

Acknowledgments

This work is financially supported by the MOST of China (2006CB601104, 2006AA03A138) and the National Natural Science Foundation of China (10574128, 10504031).

References

[1] D. Jia, B. Wu, J. Zhu, Canadian Patent No. 00100388, 2000.
[2] D. Haranath, A.F. Khan, H. Chander, Appl. Phys. Lett. 89 (2006) 91903.
[3] M.R. Royce, S. Matsuda, United States Patent 5,656,094.
[4] P.T. Diallo, P. Boutinaud, R. Mahiou, J.C. Cousseins, Phys. Stat. Sol. (a) 160 (1997) 255.
[5] W. Jia, D. Jia, T. Rodriguez, D.R. Evans, R.S. Meltzer, W.M. Yen, J. Lumin. 119–120 (2006) 13.
[6] X.M. Zhang, J.H. Zhang, X. Zhang, C. Li, S.Z. Lu, X.J. Wang, J. Lumin. 122–123 (2007) 958.
[7] X.M. Zhang, J.H. Zhang, Z.G. Nie, M.Y. Wang, X.G. Ren, X.J. Wang, Appl. Phys. Lett. 90 (2007) 151911.
[8] P. Boutinaud, E. Tomasella, A. Ennajdaoui, R. Mahiou, Thin Solid Films 515 (2006) 2316.
[9] X.M. Zhang, J.H. Zhang, X. Zhang, C. Li, Y.S. Luo, X.J. Wang, Chem. Phys. Lett. 434 (2007) 237.
[10] Z.Y. He, X.J. Wang, W.M. Yen, J. Lumin. 119–120 (2006) 309.
[11] D. Jia, R.S. Meltzer, W.M. Yen, W. Jia, X.J. Wang, Appl. Phys. Lett. 80 (2002) 1535.
[12] P. Avouris, T.N. Morgan, J. Chem. Phys. 74 (8) (1981) 4347.